RESEARCH PAPER

Design, Synthesis, Characterization, ADMET profiling and Molecular Docking Studies of Bioisosteric Derivatives as Potential CD45 Tyrosine Phosphatase Inhibitors

Komal D. Patil[1]*, Dr. Minal R. Ghante[2]

[1, 2]Department of Pharmaceutical Chemistry, Sinhgad Technical Education Society's, Smt. Kashibai Navale College of Pharmacy (Kondhwa), Savitribai Phule Pune University, Pune 411048, India.

[1]komaldpatil07@gmail.com

*Corresponding author: Komal D. Patil, komaldpatil07@gmail.com

Abstract:

Background: CD45 (PTPRC) is a receptor-type protein tyrosine phosphatase involved in the regulation of immune-cell signalling and represents a potential target for the development of novel CD45-directed therapeutic agents. TU-572 is a reported CD45 tyrosine phosphatase inhibitor and was selected as the reference scaffold for structural optimization.

Objective: The present study aimed to design, synthesize, characterize, and computationally evaluate novel bioisosteric derivatives of TU-572 as potential CD45 tyrosine phosphatase inhibitors.

Methods: A total of 24 bioisosteric derivatives were designed through systematic modification of the TU-572 scaffold, including variation of the alkoxy substituent, replacement of the methylpyridine moiety with a 7-methylenequinoline system, and incorporation of ester, ether, and hydroxyl functionalities. The synthesized compounds were characterized using FT-IR, 1H-NMR, and mass spectrometry. Molecular docking was performed against the catalytic domain of CD45 using AutoDock Vina under identical docking conditions. Binding affinity, predicted Ki, ligand efficiency, and binding interactions were evaluated. *In silico* physicochemical, pharmacokinetic, drug-likeness, and ADMET properties were assessed using SwissADME.

Key Findings: The synthesized derivatives showed satisfactory yields and spectral data consistent with their proposed structures. Five compounds, NSQD-6, NBQD-5, SBQD-4, IPQD-4, and BBQD-4, demonstrated the most favourable predicted binding affinities of −8.6, −8.5, −8.4, −8.0, and −7.7 kcal/mol, respectively, compared with −6.2 kcal/mol for TU-572. NSQD-6 exhibited the strongest predicted binding, while NBQD-5 and SBQD-4 showed favourable ligand efficiency. ADMET analysis demonstrated that improved docking affinity was not consistently associated with favourable pharmacokinetic properties.

Conclusion: NSQD-6, NBQD-5, SBQD-4, IPQD-4, and BBQD-4 were prioritized as promising computational candidates for further biological investigation. Experimental CD45 phosphatase inhibition and subsequent selectivity and cellular studies are required to establish their actual biological activity and lead potential.

Keywords: CD45; PTPRC; protein tyrosine phosphatase; TU-572; bioisosteric derivatives; molecular docking; AutoDock Vina; ADMET; ligand efficiency; drug discovery.

* *Author for Correspondence: komaldpatil07@gmail.com*

Introduction:

CD45 is a Leucocyte Common Antigen present on the cell surface of immune and haemotopoietic cells other than mature RBC's and Platelets directing towards its functional involvement in the immune response. CD45Tyrosine Phosphatase is class of Protein Tyrosine Phosphatases family and type I transmembrane protein with 3 domains such as Extracellular, transmembrane and two intracellular or cytosolic domains. **Figure 1** Explains mechanism, structure, functions and diseases directly associated with Protein CD45[1]. It is an important target in regulating immune signals or often called as "Immune signaling system". CD45 Tyrosine Phosphatase is receptor protein consisting of intracellular, extracellular and transmembrane regions. As protein acts as receptor, transmembrane portion of the protein plays an important role in activity[1-5].

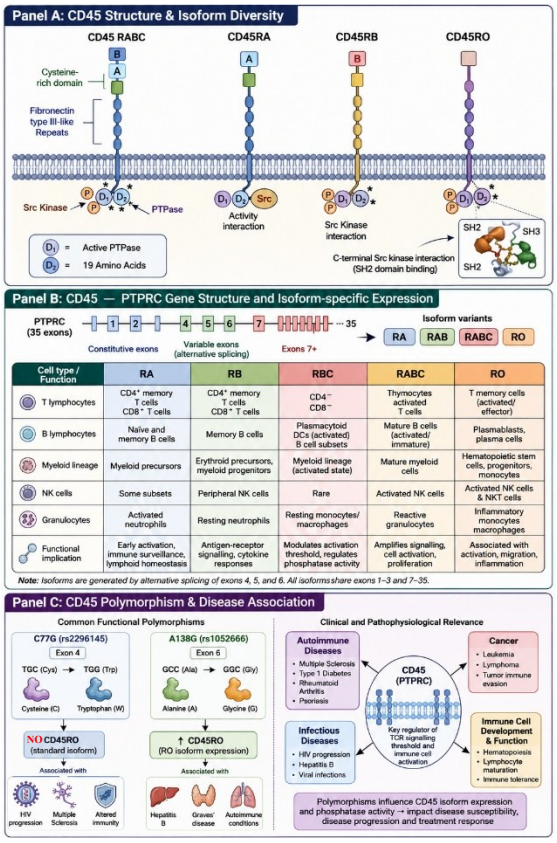

Figure 1: Mechanism, structure, functions and diseases directly associated with Protein CD45.

Unfortunately, it didn't gain much attention because more focus of the researchers was on Tyrosine Kinases over Tyrosine Phosphatase. In recent years, PTP1B is found involved into various activities such as cell differentiation and cell growth, placental development, cardiac cells growth, differentiation, etc[6]. This has changed the spectrum from kinase to phosphatase in small extent. Still, much more of Tyrosine Phosphatase are unexplored. Thus, there is an urgent need to develop new selective drugs with better safety profiles that can effectively inhibit CD45 Tyrosine Phosphatase without causing serious side effects.

The scientific literature contains large amount of data describing the synthesis, biological, pharmacological evaluation and other type of activities of CD45 Tyrosine Phosphatase inhibitors in late 20th Century[7-17]. We have screened various research articles and found TU-572 is molecule of interest. TU-572 is effective against CD45 Tyrosine Phosphatase at 0.28µM concentration. The molecule was not further investigated for other comorbidities and hence, it was decided to focus on this molecule, developing its bioisosters with various substitutions may turn promising for evaluating their effect on CD45 Tyrosine Phosphatase inhibition.

Chemical name of TU-572 is 2-[(4-methylthiopyridin-2-yl) methyl sulfinyl]-5-isopropoxybenzimidazole which is having isopropyl chain at 5th position of 2-mercapto-1H-benzimidazole ring by oxyether linkage, sulfinyl linkage joining methylated pyridine derivative with 2-mercapto-1H-benzimidazole ring. Third and fourth characteristic are pyridine ring and its involvement in various biological activities and thioether at 4th position of the ring leading to its interaction with various residues.

Materials and Methods:

Bioisosteric Design

Three changes were predominantly carried out in the structure of TU-572 and 24 molecules were optimized for further investigation. **Table No. 1** explains modifications in the structures and development of Bioisosteric derivatives of TU-572.

- Change 1: Isopropyl chain is evaluated along with n-propyl, n-butyl, sec-butyl, substitution at 5th position of 2-mercapto-1H-benzimidazole ring.
- Change 2(R2): Replacement of 2-methylpyridine ring with Quinoline ring having 7th position methylene group
- Change 3(R3): S-CH_3 at 4th position of Pyridine replaced with OH/O-ether/o-ester at 3rd position of Quinoline

Series were named based on change 1.

Synthesis and characterization

All solvents, reagents and chemicals were obtained from LOBA Chemie Pvt. Ltd., Sigma Aldrich of LR grade. These are used without further purification process. The progress of all reactions was monitored by thin layer chromatography (TLC) using Merck pre-coated silica gel G plates with a layer thickness 175-225 µm and eluent systems used were Ethyl acetate: Methanol: n-Hexane: (1:3:6 *v/v/v*). The synthesis procedure is followed with slight modifications in previously reported method[8] as described in **Scheme 1.** The step 1a is modification of 3-nitro-4-acetamidophenol into 3-nitro-4-acetamido-1-alkoxybenzene derivative. It was carried out by use of anhydrous potassium carbonate, respective alkyl bromide and acetone in reflux method. Further step 1b, 1c and 1d remains unchanged with reference procedure. The reagent was changed with 0.1M Triethylamine at 0°C in step 2 to reduce chances of decoupling of quinoline ring with mercapto-benzimidiazole ring from strong alkali such as sodium hydroxide. Further step 3 i.e. synthesis of sulfinyl derivative was achieved by m-chlorperbenzoic acid as mentioned in the reference. The final product was extracted in Ethyl acetate, with further recrystallization using ethyl acetate. The synthesis of 3-substituted-7-chloromethylquinoline was carried out using two step method as shown in **Scheme 2.** The melting point of purified compounds was carried out using open tube capillary method with thermometer having scale of 0-300°C. The 1H NMR spectra were obtained by a Bruker BioSpin GMBH spectrometer with 400 MHz in dimethyl sulfoxide (DMSO) as the solvent (Bruker Corporation, USA). The Chemical shifts are given in parts per million and are related to that of the solvent. The Shimadzu LCMS-8060XE liquid chromatography–mass spectrometer equipped with an electrospray ionization (ESI) source was employed for mass determination (Shimadzu Corporation, Kyoto, Japan). The Infrared spectra were recorded using Bruker Alpha II FTIR by KBr pellet method (Bruker Corporation, USA). The structure of the synthesized compounds was confirmed by: 1H- NMR (Nuclear Magnetic Resonance Spectroscopy), HRMS (High Resolution Mass Spectrometry) and FT-IR (Fourier Transform Infrared Spectroscopy). The structure of the synthesized compounds was confirmed by: 1H- NMR (Nuclear Magnetic Resonance Spectroscopy), HRMS (High Resolution Mass Spectrometry) and FT-IR (Fourier Transform Infrared Spectroscopy).

Table No. 1: Bioisosterically derivatives and synthesized compounds

Sr. No.	Structure ID	Series Name	R2	R3	SMILES
1	NAQD-1	N-Series (n-propyloxy)	7MQ	3-acetate*	CC(OC1=CC(C=C2)=C(N=C1)C=C2CS(C3=NC4=CC(OCCC)=CC=C4N3)=O)=O
2	NFQD-2			3-formate*	[H]C(OC1=CC(C=C2)=C(N=C1)C=C2CS(C3=NC4=CC(OCCC)=CC=C4N3)=O)=O
3	NCQD-3			3-chloroacetate*	O=C(CCl)OC1=CC(C=C2)=C(N=C1)C=C2CS(C3=NC4=CC(OCCC)=CC=C4N3)=O
4	NPQD-4			3-phenylacetate*	O=C(CC1=CC=CC=C1)OC2=CC(C=C3)=C(N=C2)C=C3CS(C4=NC5=CC(OCCC)=CC=C5N4)=O
5	NBQD-5			3-benzoate*	O=C(C1=CC=CC=C1)OC2=CC(C=C3)=C(N=C2)C=C3CS(C4=NC5=CC(OCCC)=CC=C5N4)=O
6	NSQD-6			3-salicylate*	O=C(C1=C(O)C=CC=C1)OC2=CC(C=C3)=C(N=C2)C=C3CS(C4=NC5=CC(OCCC)=CC=C5N4)=O
7	NAlQD-7			3-allyloxy**	O=S(CC1=CC(N=CC(OCC=C)=C2)=C2C=C1)C3=NC4=CC(OCCC)=CC=C4N3
8	NHQD-8			3-hydroxy***	OC1=CC(C=C2)=C(N=C1)C=C2CS(C3=NC4=CC(OCCC)=CC=C4N3)=O
9	IAQD-1	I-Series (isopropyloxy)		3-acetate*	CC(C)OC1=CC=C(NC(S(CC2=CC(N=CC(OC(C)=O)=C3)=C3C=C2)=O)=N4)C4=C1
10	IFQD-2			3-formate*	CC(C)OC1=CC=C(NC(S(CC2=CC(N=CC(OC([H])=O)=C3)=C3C=C2)=O)=N4)C4=C1
11	ICQD-3			3-chloroacetate*	CC(C)OC1=CC=C(NC(S(CC2=CC(N=CC(OC(CCl)=O)=C3)=C3C=C2)=O)=N4)C4=C1
12	IPQD-4			3-phenylacetate*	CC(C)OC1=CC=C(NC(S(CC2=CC(N=CC(OC(CC3=CC=CC=C3)=O)=C4)=C4C=C2)=O)=N5)C5=C1
13	IIQD-5			3-isopropoxy**	CC(C)OC1=CC=C(NC(S(CC2=CC(N=CC(OC(C)C)=C3)=C3C=C2)=O)=N4)C4=C1
14	IHQD-6			3-hydroxy***	OC1=CC(C=C2)=C(N=C1)C=C2CS(C3=NC4=CC(OC(C)C)=CC=C4N3)=O
15	BAQD-1	B-Series (butyloxy)		3-acetate*	CC(OC1=CC(C=C2)=C(N=C1)C=C2CS(C3=NC4=CC(OCCCC)=CC=C4N3)=O)=O
16	BFQD-2			3-formate*	[H]C(OC1=CC(C=C2)=C(N=C1)C=C2CS(C3=NC4=CC(OCCCC)=CC=C4N3)=O)=O
17	BCQD-3			3-chloroacetate*	O=C(CCl)OC1=CC(C=C2)=C(N=C1)C=C2CS(C3=NC4=CC(OCCCC)=CC=C4N3)=O
18	BBQD-4			3-benzoate*	O=C(C1=CC=CC=C1)OC2=CC(C=C3)=C(N=C2)C=C3CS(C4=NC5=CC(OCCCC)=CC=C5N4)=O
19	SAQD-1	S-Series (sec-butyloxy)		3-acetate*	CC(OC1=CC(C=C2)=C(N=C1)C=C2CS(C3=NC4=CC(OC(C)CC)=CC=C4N3)=O)=O
20	SFQD-2			3-formate*	[H]C(OC1=CC(C=C2)=C(N=C1)C=C2CS(C3=NC4=CC(OC(C)CC)=CC=C4N3)=O)=O
21	SCQD-3			3-chloroacetate*	O=C(CCl)OC1=CC(C=C2)=C(N=C1)C=C2CS(C3=NC4=CC(OC(C)CC)=CC=C4N3)=O
22	SBQD-4			3-benzoate*	O=C(C1=CC=CC=C1)OC2=CC(C=C3)=C(N=C2)C=C3CS(C4=NC5=CC(OC(C)CC)=CC=C5N4)=O
23	SIOD-5			3-isopropoxy**	CC(C)OC1=CC(C=C2)=C(N=C1)C=C2CS(C3=NC4=CC(OC(C)CC)=CC=C4N3)=O
24	SAlQD-6			3-allyloxy**	O=S(CC1=CC(N=CC(OCC=C)=C2)=C2C=C1)C3=NC4=CC(OC(C)CC)=CC=C4N3

Notations: 7MQ:7-methylene Quinoline ring *- Ester derivative **- Ether derivative ***- Phenol

Scheme 1: General Synthetic Route for the Preparation of Novel TU-572-Based Bioisosteric Derivatives

Scheme 2: General Synthetic Route for the Preparation of 7-Chloromethylquinoline Derivatives

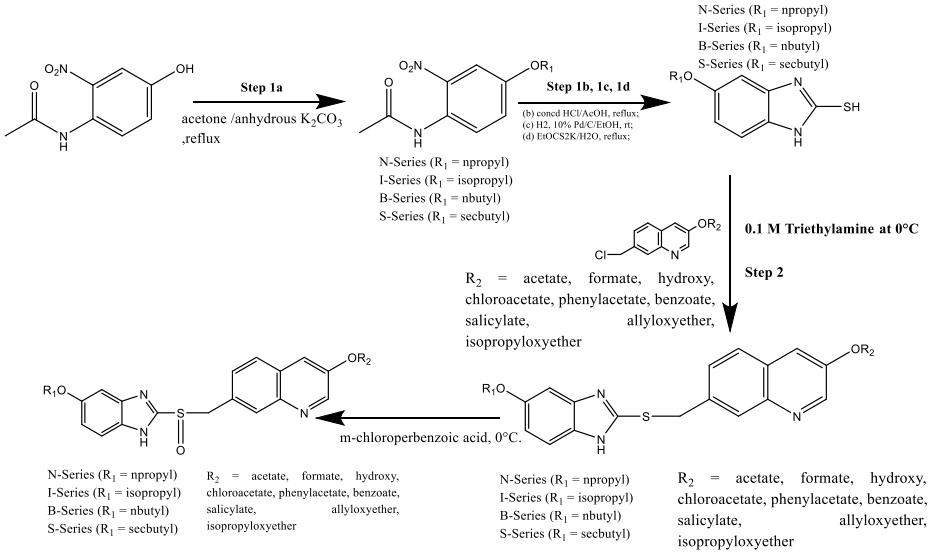

Scheme 2: General Synthetic Route for the Preparation of 7-Chloromethylquinoline Derivatives

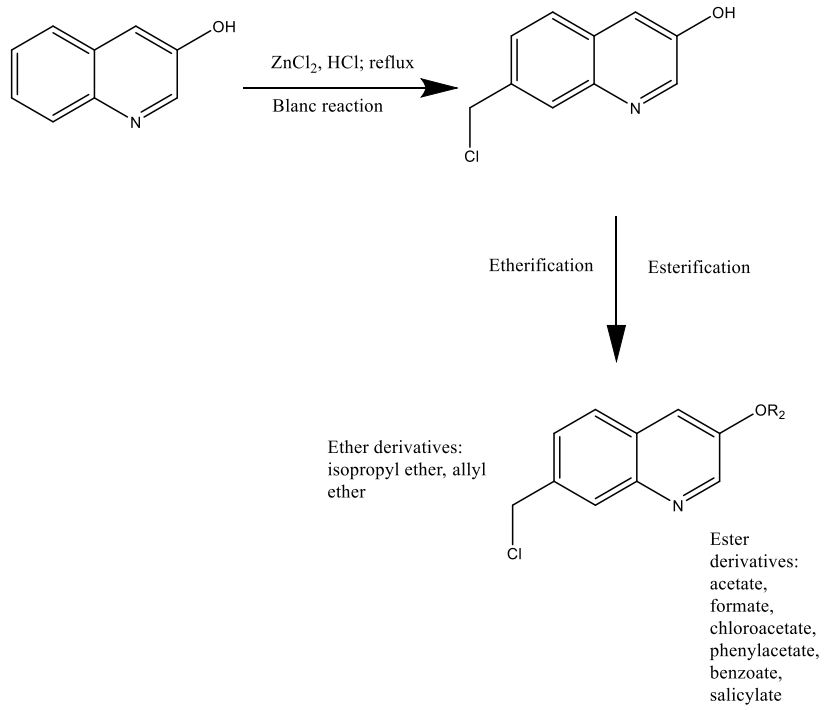

Molecular docking

a) Protein preparation[18]: The three-dimensional crystal structure of CD45 tyrosine phosphatase was obtained from the Protein Data Bank **(PDB ID: 1YGU).** The protein is characterised using X-ray Diffraction with the resolution of 2.90. CD45 tyrosine phosphatase is hydrous class of enzyme with EC number EC3.1.3.48 which is expressed in *Escherichia coli* BL21 with modified residue of PTR (O-phosphotyrosine). This is 4 amino acid containing peptide is ligand attached to the protein. CD45 is transmembrane receptor protein with extracellular, transmembrane and cytosolic portions. The amino acid chain [608-890] was selected based on the literature information, employing its functionality and BIOVIA Discovery Studio 2024 was employed further for protein structure preparation enabling it for molecular docking. Removal of water molecule, heteroatom and Tyrosine residue ligand and addition of polar hydrogen atoms, correction of missing residues or repair of residual atoms, further energy mineralization and structural optimisation to make it ready in appropriate format for docking using BIOVIA Discovery Studio 2024 and AutoDock Vina tools[19-20].

b) Ligand preparation: Synthesised compounds and reference molecule were drawn using chemdraw[21] and converted into three-dimensional structures. The resulting structures were subjected to geometry optimisation and energy mineralization using an appropriate molecular mechanic's force fields prior to molecular docking. The prepared compounds were subsequently docked against the catalytic domain of CD45 using Autodock Vina to evaluate their predicted binding affinities and interactions within the active-site regions.

c) Docking protocol and understanding of the docking conditions: The docking grid was entered on the catalytic binding pocket using the co-ordinates X= 16.310784, Y = -14.708432 and Z = 59.134378. A grid -box dimension of 40 x 40 x 40Å was utilized to provide sufficiently occupying active site cavity and surrounding residues with optimal interactions. Docking studies were performed under identical conditions for all selected compounds, and the resulting binding affinities were recorded in kcal/mol. Ligand re-docking is not possible due to presence of peptide residue at the active site rather than small inhibitors, comparison of predicted binding mode of reference molecules with ligands were analyzed to understand the binding efficiency of the molecules.

The predicted inhibitory constant was determined using formula given below[22]:

$$pKi = 10\left(\frac{\Delta G}{1.366}\right)$$

Where ΔG= binding energy (Kcal/mol) and pKi is expressed in μM.

The ligand efficiency was determined using formula given below[23]:

$$LE = -\frac{\Delta G}{NHA}$$

Where ΔG= binding energy (Kcal/mol) and NHA = Number of heavy atoms in the ligand

The docked conformations were ranked according to binding affinity, pKi and LE values and the binding modes of the top-ranked compounds were

subsequently examined in comparison to the reference molecule.

ADMET and drug likeness evaluation:

The drug-likeness, pharmacokinetics and toxicity profile of the synthesized compounds and reference molecule were predicted using the Swiss ADME[24] online platform.

Results:

Design and Synthesis of bioisosteric derivatives

A bioisosteric modification strategy was adopted using TU-572 as the parent/reference scaffold. Three principal structural modifications were introduced: variation of the alkoxy substituent at the benzimidazole ring, replacement of the methylpyridine moiety with a quinoline system containing a 7-methylene linker, and modification of the quinoline substituent through ester, ether, and hydroxyl functionalities. A total of 24 derivatives were designed and optimized for further investigation. The synthesized molecules were categorized into N-series, I-series, B-series, and S-series according to the alkoxy substituent incorporated into the benzimidazole ring. The synthesized compounds were obtained as crystalline, amorphous, waxy, or solid materials with reported yields ranging from approximately 70.2% to 88.6%. The compounds exhibited distinct melting points and Rf values, supporting differences in their physicochemical characteristics. Representative compounds such as NSQD-6, NBQD-5, and SBQD-4 were obtained in yields of 79.3%, 79.2%, and 81.2%, respectively, whereas several other derivatives also showed yields above 80%. **Table 2** gives information about the physicochemical properties of the compounds.

Spectroscopic and structural characterization

The synthesized derivatives were characterized using FT-IR, 1H NMR, and mass spectrometry. The spectral data were consistent with the proposed structures. The compounds generally exhibited N–H stretching bands in the region of approximately 3340–3422 cm^{-1}, together with characteristic aromatic C–H, aliphatic C–H, aromatic C=C, C–O, S=O, and C–S/S–CH_2 absorptions. Ester-containing derivatives showed characteristic carbonyl absorption bands in the region of approximately 1690–1774 cm^{-1}. Hydroxy-containing derivatives exhibited additional O–H absorption bands. The 1H NMR spectra further supported the proposed structures. A characteristic benzimidazole N–H signal was consistently observed around δ 11-12 ppm. The quinoline H-C2 proton generally appeared around δ 8.46–8.62 ppm. The $SOCH_2$ group was observed around δ 4.54 ppm, while signals attributable to the respective alkoxy, ester, hydroxyl, and substituted aromatic groups were observed at the expected chemical-shift regions. For example, NSQD-6 displayed an additional hydroxyl proton at δ 10.58 ppm, whereas NAlQD-7 showed characteristic allylic signals between approximately δ 4.73 and 6.03 ppm. Mass spectral data were also in agreement with the proposed molecular structures. The experimentally observed molecular-ion-related peaks were generally close to their corresponding calculated molecular masses, providing additional support for successful synthesis of the targeted derivatives.

The characterization data of all series is given below:

7-(((5-propoxy-1H-benzo[d]imidazol-2-yl) sulfinyl) methyl) quinolin-3-yl acetate (NAQD-1):

IR (KBr): 3394 (str, N–H), 3065, 3038, 3013 (str, aromatic C–H), 2933 (str, =C–H/aliphatic C–H), 1704 (str, ester C=O), 1654 (str, C=N/conjugated C=C), 1597, 1553 (str, aromatic C=C), 1467 (def, CH_2/aromatic skeletal), 1387, 1346, 1316 (def, CH_2/CH), 1293, 1229, 1211 (str, ester/aryl C–O), 1163, 1143, 1117, 1071 (str, S=O/C–O–C), 998 (oop, =C–H), 905 (oop, =C–H), 869, 852, 818, 737 (oop, aromatic C–H), 656, 615 cm^{-1} (str, C–S/S–CH_2); ^1H NMR (400 MHz, DMSO): δ 11.37 (bs, 1H, NH), 8.61–8.62 (d, 1H, H-C2 of quinoline), 6.97–7.90 (m, 7H, Ar-H), 4.54 (bs, 2H, $SOCH_2$), 3.93–3.95 (t, 2H, OCH_2), 2.26 (bs, 3H, $COCH_3$), 1.80–1.83 (m, 2H, CH_2-CH_3), 1.10–1.13 (t, 3H, CH_3); m/z = 424.80 $(M+H)^+$ Theoretical Calculated= 423.49

7-(((5-propoxy-1H-benzo[d]imidazol-2-yl) sulfinyl) methyl) quinolin-3-yl formate (NFQD-2):

IR (KBr): 3373 (str, N–H), 3063 (str, aromatic C–H), 2951 (str, =C–H/aliphatic C–H), 1704 (str, ester C=O), 1596, 1552 (str, aromatic C=C), 1466 (def, CH_2/aromatic skeletal), 1366, 1348 (def, CH_2/CH), 1271, 1210 (str, ester/aryl C–O), 1134 (str, S=O/C–O–C), 995 (oop, =C–H), 902 (oop, =C–H), 869, 819, 738 (oop, aromatic C–H), 664, 615 cm^{-1} (str, C–S/S–CH_2); ^1H NMR (400 MHz, DMSO): δ 11.37 (bs, 1H, NH), 8.56–8.57 (d, 1H, H-C2 of quinoline), 8.36 (bs, 1H, CHO), 6.97–7.88 (m, 7H, Ar-H), 4.54 (bs, 2H, $SOCH_2$), 3.93–3.95 (t, 2H, OCH_2), 1.79–1.84 (m, 2H, CH_2-CH_3), 1.10–1.13 (t, 3H, CH_3); m/z = 410.20 $(M+H)^+$ Theoretical Calculated= 409.46

7-(((5-propoxy-1H-benzo[d]imidazol-2-yl) sulfinyl) methyl) quinolin-3-yl 2-chloroacetate (NCQD-3):

IR (KBr): 3391 (str, N–H), 3015 (str, aromatic C–H), 2927 (str, =C–H/aliphatic C–H), 1731 (str, ester C=O), 1693 (str, C=N/conjugated C=C), 1596, 1553 (str, aromatic C=C), 1465 (def, CH_2/aromatic skeletal), 1388, 1348 (def, CH_2/CH), 1268, 1215 (str, ester/aryl C–O), 1134 (str, S=O/C–O–C), 996 (oop, =C–H), 906 (oop, =C–H), 864, 817, 741 (oop, aromatic C–H), 663, 616 cm^{-1} (str, C–Cl/C–S/S–CH_2); ^1H NMR (400 MHz, DMSO): δ 11.38 (bs, 1H, NH), 8.60 (d, 1H, H-C2 of quinoline), 6.97–7.90 (m, 7H, Ar-H), 4.54 (bs, 2H, $SOCH_2$), 4.24 (bs, 2H, CH_2Cl), 3.93–3.95 (t, 2H, OCH_2), 1.79–1.86 (m, 2H, CH_2-CH_3), 1.10–1.13 (t, 3H, CH_3); m/z = 460.10 $(M+2)^+$ Theoretical Calculated= 457.93

7-(((5-propoxy-1H-benzo[d]imidazol-2-yl) sulfinyl) methyl) quinolin-3-yl 2-phenylacetate (NPQD-4):

IR (KBr): 3397 (str, N–H), 3063 (str, aromatic C–H), 2947 (str, =C–H/aliphatic C–H), 1704 (str, ester C=O), 1693 (str, C=N/conjugated C=C), 1596, 1554 (str, aromatic C=C), 1467 (def, CH_2/aromatic skeletal), 1388, 1343 (def, CH_2/CH), 1253, 1209 (str, ester/aryl C–O), 1137, 1072 (str, S=O/C–O–C), 997 (oop, =C–H), 903 (oop, =C–H), 868, 820, 738 (oop, aromatic C–H), 664, 615 cm^{-1} (str, C–S/S–CH_2); ^1H NMR (400 MHz, DMSO): δ 11.37 (bs, 1H, NH), 8.57 (d, 1H, H-C2 of quinoline), 6.97–7.89 (m, 12H, Ar-H), 4.54 (bs, 2H, $SOCH_2$), 3.93–3.95 (t, 2H, OCH_2), 3.49 (bs, 2H, CH_2), 1.79–1.85 (m, 2H, CH_2-CH_3), 1.10–1.13 (t, 3H, CH_3); m/z = 500.20 $(M+H)^+$ Theoretical Calculated= 499.60

7-(((5-propoxy-1H-benzo[d]imidazol-2-yl) sulfinyl) methyl) quinolin-3-yl benzoate (NBQD-5):

IR (KBr): 3403 (str, N–H), 3066 (str, aromatic C–H), 2945 (str, =C–H/aliphatic C–H), 1731 (str, ester C=O), 1658 (str, C=N/conjugated C=C), 1597, 1534 (str, aromatic C=C), 1464 (def, CH_2/aromatic skeletal), 1388, 1345 (def, CH_2/CH), 1275, 1215 (str, ester/aryl C–O), 1181, 1137,

1072 (str, S=O/C–O–C), 946 (oop, =C–H), 907 (oop, =C–H), 869, 744 (oop, aromatic C–H), 667, 619 cm^{-1} (str, C–S/S–CH_2); ^1H NMR (400 MHz, DMSO): δ 11.37 (bs, 1H, NH), 8.60 (d, 1H, H-C2 of quinoline), 8.11–8.13 (m, 2H, Ar-H), 6.97–7.88 (m, 10H, Ar-H), 4.54 (bs, 2H, $SOCH_2$), 3.93–3.95 (t, 2H, OCH_2), 1.79–1.85 (m, 2H, CH_2-CH_3), 1.10–1.13 (t, 3H, CH_3); m/z = 486.30 $(M+H)^+$ Theoretical Calculated= 485.56

7-(((5-propoxy-1H-benzo[d]imidazol-2-yl) sulfinyl) methyl) quinolin-3-yl 2-hydroxybenzoate (NSQD-6):

IR (KBr): 3408, 3386 (str, O–H/N–H), 3015 (str, aromatic C–H), 2943 (str, =C–H/aliphatic C–H), 1704 (str, ester C=O), 1693 (str, C=N/conjugated C=C), 1590, 1555 (str, aromatic C=C), 1493, 1461 (def, CH_2/aromatic skeletal), 1366, 1343 (def, CH_2/CH), 1277, 1214 (str, ester/aryl C–O), 1138 (str, S=O/C–O–C), 995 (oop, =C–H), 904 (oop, =C–H), 868, 818, 737 (oop, aromatic C–H), 696, 669, 615 cm^{-1} (str, C–S/S–CH_2); ^1H NMR (400 MHz, DMSO): δ 11.37 (bs, 1H, NH), 10.58 (bs, 1H, OH), 8.60–8.61 (d, 1H, H-C2 of quinoline), 6.94–7.89 (m, 11H, Ar-H), 4.54 (bs, 2H, $SOCH_2$), 3.93–3.95 (t, 2H, OCH_2), 1.79–1.85 (m, 2H, CH_2-CH_3), 1.10–1.13 (t, 3H, CH_3); m/z = 502.8 $(M+H)^+$ Theoretical Calculated= 501.56

3-(allyloxy)-7-(((5-propoxy-1H-benzo[d]imidazol-2-yl) sulfinyl) methyl) quinoline (NAlQD-7):

IR (KBr): 3364 (str, N–H), 3015 (str, aromatic C–H), 2930 (str, =C–H/aliphatic C–H), 1595, 1551 (str, aromatic C=C), 1466 (def, CH_2/aromatic skeletal), 1387 (def, CH_2/CH), 1273, 1216 (str, ether/aryl C–O), 1163, 1119, 1074 (str, S=O/C–O–C), 996 (oop, allylic =C–H), 902 (oop, =C–H), 870, 817, 737 (oop, aromatic C–H), 667, 615 cm^{-1} (str, C–S/S–CH_2); ^1H NMR (400 MHz, DMSO): δ 11.37 (bs, 1H, NH), 8.46–8.47 (d, 1H, H-C2 of quinoline), 6.99–7.87 (m, 7H, Ar-H), 5.99–6.03 (m, 1H, CH of allyl), 5.47 (m, 1H, CH_2 of allyl), 5.11 (m, 1H, CH_2 of allyl), 4.73 (d, 2H, OCH_2-$CH=CH_2$), 4.54 (bs, 2H, $SOCH_2$), 3.93–3.95 (t, 2H, OCH_2), 1.79–1.85 (m, 2H, CH_2-CH_3), 1.10–1.13 (t, 3H, CH_3); m/z = 422.8 $(M+H)^+$ Theoretical Calculated= 421.52

7-(((5-propoxy-1H-benzo[d]imidazol-2-yl) sulfinyl) methyl) quinolin-3-ol (NHQD-8):

IR (KBr): 3408, 3385 (str, O–H/N–H), 3066, 3014 (str, aromatic C–H), 2926 (str, =C–H/aliphatic C–H), 1655 (str, C=N/conjugated C=C), 1597, 1534 (str, aromatic C=C), 1465 (def, CH_2/aromatic skeletal), 1386, 1343, 1315 (def, CH_2/CH), 1266, 1208 (str, ether/aryl C–O), 1137 (str, S=O/C–O–C), 995 (oop, =C–H), 904 (oop, =C–H), 851, 816, 736 (oop, aromatic C–H), 665, 615 cm^{-1} (str, C–S/S–CH_2); ^1H NMR (400 MHz, DMSO): δ 11.37 (bs, 1H, NH), 8.53 (d, 1H, H-C2 of quinoline), 8.37 (d, 1H, OH), 6.97–7.90 (m, 7H, Ar-H), 4.54 (bs, 2H, $SOCH_2$), 3.93–3.95 (t, 2H, OCH_2), 1.79–1.84 (m, 2H, CH_2-CH_3), 1.10–1.13 (t, 3H, CH_3); m/z = 382.50 $(M+H)^+$ Theoretical Calculated= 381.45

7-(((5-isopropoxy-1H-benzo[d]imidazol-2-yl) sulfinyl) methyl) quinolin-3-yl acetate (IAQD-1):

IR (KBr): 3416 (str, N–H), 3064 (str, aromatic C–H), 2951 (str, =C–H/aliphatic C–H), 1693 (str, ester C=O), 1552, 1504 (str, aromatic C=C), 1467 (def, CH_2/aromatic skeletal), 1378, 1341 (def, CH_2/CH), 1277, 1212 (str, ester/aryl C–O), 1177, 1140, 1096, 1066, 1023 (str, S=O/C–O–C), 988 (oop, =C–H), 951 (oop, =C–H), 885, 855, 748 (oop, aromatic C–H), 654, 616 cm^{-1} (str, C–S/S–CH_2); ^1H NMR (400 MHz, DMSO): δ 11.37 (bs, 1H, NH), 8.61–8.62 (d, 1H, H-C2 of quinoline), 6.97–7.89 (m, 7H, Ar-H), 4.54 (bs, 2H, $SOCH_2$), 4.01–4.05 (m, 1H, OCH), 2.26 (bs, 3H, $COCH_3$), 1.29–1.30 (d, 6H, CH_3); m/z = 424.60 $(M+H)^+$ Theoretical Calculated= 423.49

7-(((5-isopropoxy-1H-benzo[d]imidazol-2-yl) sulfinyl) methyl) quinolin-3-yl formate (IFQD-2):

IR (KBr): 3392 (str, N–H), 3063 (str, aromatic C–H), 2937 (str, =C–H/aliphatic C–H), 1724 (str, ester C=O), 1652 (str, C=N/conjugated C=C), 1597, 1555 (str, aromatic C=C), 1468 (def, CH_2/aromatic skeletal), 1383, 1345 (def, CH_2/CH), 1265, 1218 (str, ester/aryl C–O), 1136, 1117, 1073 (str, S=O/C–O–C), 996, 954 (oop, =C–H), 904 (oop, =C–H), 872, 832, 739 (oop, aromatic C–H), 665, 614 cm^{-1} (str, C–S/S–CH_2); ^{1}H NMR (400 MHz): δ 11.37 (bs, 1H, NH), 8.56–8.57 (d, 1H, H-C2 of quinoline), 8.36 (bs, 1H, CHO), 6.97–7.88 (m, 7H, Ar-H), 4.61–4.67 (m, 1H, OCH), 4.54 (bs, 2H, $SOCH_2$), 1.29–1.30 (d, 6H, CH_3); m/z = 410.70 $(M+H)^+$ Theoretical Calculated= 409.46

7-(((5-isopropoxy-1H-benzo[d]imidazol-2-yl) sulfinyl) methyl) quinolin-3-yl 2-chloroacetate (ICQD-3):

IR (KBr): 3394 (str, N–H), 3055 (str, aromatic C–H), 2951 (str, =C–H/aliphatic C–H), 1690 (str, ester C=O), 1599 (str, C=N/conjugated C=C), 1552, 1502 (str, aromatic C=C), 1469 (def, CH_2/aromatic skeletal), 1381, 1343 (def, CH_2/CH), 1277, 1212 (str, ester/aryl C–O), 1177, 1136, 1113, 1066, 1013 (str, S=O/C–O–C), 995 (oop, =C–H), 951 (oop, =C–H), 885, 830, 752 (oop, aromatic C–H), 672, 635, 612 cm^{-1} (str, C–Cl/C–S/S–CH_2); ^{1}H NMR (400 MHz, DMSO): δ 11.37 (bs, 1H, NH), 8.58 (d, 1H, H-C2 of quinoline), 6.96–7.89 (m, 7H, Ar-H), 4.61–4.66 (m, 1H, OCH), 4.54 (bs, 2H, $SOCH_2$), 4.24 (bs, 2H, CH_2Cl), 1.29–1.30 (d, 6H, CH_3); m/z = 460.00 $(M+2)^+$ Theoretical Calculated= 457.93

7-(((5-isopropoxy-1H-benzo[d]imidazol-2-yl) sulfinyl) methyl) quinolin-3-yl 2-phenylacetate (IPQD-4):

IR (KBr): 3408 (str, N–H), 3128 (str, aromatic C–H), 2949 (str, =C–H/aliphatic C–H), 1704 (str, ester C=O), 1655 (str, C=N/conjugated C=C), 1595, 1558 (str, aromatic C=C), 1498, 1468, 1440 (def, CH_2/aromatic skeletal), 1379, 1342 (def, CH_2/CH), 1264, 1222 (str, ester/aryl C–O), 1140, 1114, 1066 (str, S=O/C–O–C), 996, 948 (oop, =C–H), 904 (oop, =C–H), 874, 831, 748 (oop, aromatic C–H), 668, 613 cm^{-1} (str, C–S/S–CH_2); ^{1}H NMR (400 MHz, DMSO): δ 11.37 (bs, 1H, NH), 8.50 (d, 1H, H-C2 of quinoline), 6.97–7.89 (m, 12H, Ar-H), 4.61–4.67 (m, 1H, OCH), 4.54 (bs, 2H, $SOCH_2$), 3.49 (bs, 2H, $OCOCH_2$), 1.29–1.30 (d, 6H, CH_3); m/z = 500.00 $(M+H)^+$ Theoretical Calculated= 499.60

3-isopropoxy-7-(((5-isopropoxy-1H-benzo[d]imidazol-2-yl) sulfinyl) methyl) quinoline (IIQD-5):

IR (KBr): 3393 (str, N–H), 3066 (str, aromatic C–H), 2979 (str, =C–H/aliphatic C–H), 1600, 1560, 1503 (str, aromatic C=C), 1468, 1418 (def, CH_2/aromatic skeletal), 1392, 1345, 1316 (def, CH_2/CH), 1292, 1270, 1229, 1212 (str, aryl C–O), 1181, 1142, 1108 (str, S=O/C–O–C), 994 (oop, =C–H), 906 (oop, =C–H), 872, 850, 821, 753, 740 (oop, aromatic C–H), 670, 615 cm^{-1} (str, C–S/S–CH_2); ^{1}H NMR (400 MHz, DMSO): δ 11.73 (bs, 1H, NH), 8.49 (d, 1H, H-C2 of quinoline), 6.98–7.81 (m, 7H, Ar-H), 4.55–4.66 (m, 2H, OCH), 4.54 (bs, 2H, $SOCH_2$), 1.29–1.30 (d, 12H, CH_3); m/z = 424.30 (M+H)+ Theoretical Calculated= 423.53

7-(((5-isopropoxy-1H-benzo[d]imidazol-2-yl) sulfinyl) methyl) quinolin-3-ol (IHQD-6):

IR (KBr): 3416, 3394 (str, O–H/N–H), 3067 (str, aromatic C–H), 2951 (str, =C–H/aliphatic C–H), 1596, 1552 (str, aromatic C=C), 1467 (def, CH_2/aromatic skeletal), 1386, 1348 (def, CH_2/CH), 1272, 1215 (str, aryl C–O), 1143, 1071 (str, S=O/C–O–C), 999, 952 (oop, =C–H), 904 (oop, =C–H), 870, 821, 737 (oop, aromatic C–H), 667, 617 cm^{-1} (str, C–S/S–CH_2); ^{1}H NMR (400 MHz, DMSO): δ 11.37 (bs, 1H, NH), 8.53 (d, 1H, H-C2 of quinoline), 8.37 (m, 1H, 3-

OH of quinoline), 6.97–7.90 (m, 7H, Ar-H), 4.61–4.67 (m, 1H, OCH), 4.54 (bs, 2H, $SOCH_2$), 1.29–1.30 (d, 6H, CH_3); m/z = 382.70 $(M+H)^+$ Theoretical Calculated= 381.45

7-(((5-butoxy-1H-benzo[d]imidazol-2-yl) sulfinyl) methyl) quinolin-3-yl acetate (BAQD-1):

IR (KBr): 3373 (str, N–H), 3067 (str, aromatic C–H), 2920 (str, aliphatic C–H), 1720 (str, ester C=O), 1693 (str, C=N/conjugated C=C), 1597, 1534 (str, aromatic C=C), 1460 (def, CH_2/aromatic skeletal), 1387, 1343 (def, CH_2/CH), 1273, 1214 (str, ester/aryl C–O), 1174, 1136 (str, S=O/C–O–C), 997 (oop, allylic =C–H), 912 (oop, =C–H), 865, 817, 742 (oop, aromatic C–H), 677, 619 cm^{-1} (str, C–S/S–CH_2); ^1H NMR (400 MHz, DMSO**):** δ 11.37 (bs, 1H, NH), 8.61–8.62 (d, 1H, H-C2 of quinoline), 6.97–7.89 (m, 7H, Ar-H), 4.54 (bs, 2H, $SOCH_2$), 3.99–4.02 (t, 2H, OCH_2), 2.26 (bs, 3H, $COCH_3$), 1.77–1.79 (m, 2H, CH-CH_2-CH_3), 1.45–1.47 (m, 2H, CH-CH_3), 0.96–0.99 (t, 3H, CH_3); m/z = 438.10 $(M+H)^+$ Theoretical Calculated= 437.5

7-(((5-butoxy-1H-benzo[d]imidazol-2-yl) sulfinyl) methyl) quinolin-3-yl formate (BFQD-2):

IR (KBr): 3340 (str, N–H), 3063 (str, aromatic C–H), 2943 (str, =C–H), 2831 (str, aliphatic C–H), 1720 (str, ester C=O), 1693 (str, C=N/conjugated C=C), 1599, 1556 (str, aromatic C=C), 1467 (def, CH_2/aromatic skeletal), 1379 (def, CH_2/CH), 1292, 1253 (str, ester/aryl C–O), 1115, 1021 (str, S=O/C–O–C), 998 (oop, allylic =C–H), 906 (oop, =C–H), 751 (oop, aromatic C–H), 670 cm^{-1} (str, C–S/S–CH_2); ^1H NMR (400 MHz, DMSO): δ 11.37 (bs, 1H, NH), 8.56–8.57 (d, 1H, H-C2 of quinoline), 8.36 (bs, 1H, CHO), 6.97–7.88 (m, 7H, Ar-H), 4.54 (bs, 2H, $SOCH_2$), 3.99–4.02 (t, 2H, OCH_2), 1.75–1.81 (m, 2H, CH-CH_2-CH_3), 1.43–1.48 (m, 2H, CH-CH_3), 0.96–0.99 (t, 3H, CH_3); m/z = 424.00 $(M+H)^+$ Theoretical Calculated= 423.49

7-(((5-butoxy-1H-benzo[d]imidazol-2-yl) sulfinyl) methyl) quinolin-3-yl 2-chloroacetate (BCQD-3):

IR (KBr): 3416, 3375, 3278, 3178, 3128 (str, N–H), 3055 (str, aromatic C–H), 2951 (str, =C–H), 2855 (str, aliphatic C–H), 1774, 1724 (str, ester C=O), 1676 (str, C=N/conjugated C=C), 1595, 1552 (str, aromatic C=C), 1469 (def, CH_2/aromatic skeletal), 1390, 1340 (def, CH_2/CH), 1292, 1219 (str, ester/aryl C–O), 1140 (str, S=O/C–O–C), 994 (oop, allylic =C–H), 908 (oop, =C–H), 826, 740 (oop, aromatic C–H), 669 cm^{-1} (str, C-Cl/C–S/S–CH_2); ^1H NMR (400 MHz, DMSO): δ 11.37 (bs, 1H, NH), 8.58–8.59 (d, 1H, H-C2 of quinoline), 6.97–7.89 (m, 7H, Ar-H), 4.54 (bs, 2H, $SOCH_2$), 4.24 (bs, 2H, CH_2Cl), 3.99–4.02 (t, 2H, OCH_2), 1.75–1.78 (m, 2H, CH-CH_2-CH_3), 1.43–1.50 (m, 2H, CH-CH_3), 0.96–0.99 (t, 3H, CH_3); m/z = 473.85 $(M+2)^+$ Theoretical Calculated= 471.96

7-(((5-butoxy-1H-benzo[d]imidazol-2-yl) sulfinyl) methyl) quinolin-3-yl benzoate (BBQD-4):

IR (KBr): 3422 (str, N–H), 3140 (str, aromatic C–H), 2934 (str, =C–H/aliphatic C–H), 1724 (str, ester C=O), 1673 (str, C=N/conjugated C=C), 1595, 1553 (str, aromatic C=C), 1464 (def, CH_2/aromatic skeletal), 1388, 1344, 1310 (def, CH_2/CH), 1270, 1213 (str, ester/aryl C–O), 1131 (str, S=O/C–O–C), 995 (oop, allylic =C–H), 906 (oop, =C–H), 851, 814, 738 (oop, aromatic C–H), 664, 619 cm^{-1} (str, C–S/S–CH_2); ^1H NMR (400 MHz, DMSO): δ 11.37 (bs, 1H, NH), 8.60 (d, 1H, H-C2 of quinoline), 8.11–8.13 (m, 2H, Ar-H), 6.97–7.88 (m, 10H, Ar-H), 4.54 (bs, 2H, $SOCH_2$), 3.99–4.02 (t, 2H, OCH_2), 1.75–1.81 (m, 2H, CH-CH_2-CH_3), 1.43–1.50 (m, 2H, CH-CH_3), 0.96–0.99 (t, 3H, CH_3); m/z = 500.60 $(M+H)^+$ Theoretical Calculated= 499.59

7-(((5-(sec-butoxy)-1H-benzo[d]imidazol-2-yl) sulfinyl) methyl) quinolin-3-yl acetate (SAQD-1):

IR (KBr): 3392 (str, N–H), 3015 (str, aromatic C–H), 2963, 2884 (str, =C–H/aliphatic C–H), 1704 (str, ester C=O), 1587, 1553 (str, aromatic C=C), 1421 (def, CH_2/aromatic skeletal), 1392 (def, CH_2/CH), 1261, 1215 (str, ester/aryl C–O), 1109 (str, S=O/C–O–C), 996 (oop, =C–H), 870, 807, 746 (oop, aromatic C–H), 664, 616 cm^{-1} (str, C–S/S–CH_2); ^1H NMR (400 MHz, DMSO): δ 11.37 (bs, 1H, NH), 8.62 (d, 1H, H-C2 of quinoline), 6.94–7.90 (m, 7H, Ar-H), 4.54 (bs, 2H, $SOCH_2$), 4.25–4.28 (m, 1H, OCH), 2.26 (bs, 3H, $COCH_3$), 1.50–1.55 (m, 2H, CH_2-CH_3), 1.25–1.27 (d, 3H, CH_3-CH-O), 0.95–0.99 (m, 3H, CH_3); m/z = 438.9 $(M+H)^+$ Theoretical Calculated= 437.51

7-(((5-(sec-butoxy)-1H-benzo[d]imidazol-2-yl) sulfinyl) methyl) quinolin-3-yl formate (SFQD-2):

IR (KBr): 3406 (str, N–H), 3010 (str, aromatic C–H), 2927 (str, =C–H), 2884 (str, aliphatic C–H), 1728 (str, ester C=O), 1679 (str, C=N/conjugated C=C), 1595, 1553 (str, aromatic C=C), 1465 (def, CH_2/aromatic skeletal), 1389, 1345, 1313 (def, CH_2/CH), 1267, 1212 (str, ester/aryl C–O), 1171, 1136 (str, S=O/C–O–C), 997 (oop, allylic =C–H), 905 (oop, =C–H), 852, 816, 739 (oop, aromatic C–H), 663, 615 cm^{-1} (str, C–S/S–CH_2); ^1H NMR (400 MHz, DMSO): δ 11.37 (bs, 1H, NH), 8.57 (d, 1H, H-C2 of quinoline), 8.36 (bs, 1H, CHO), 6.94–7.89 (m, 7H, Ar-H), 4.54 (bs, 2H, $SOCH_2$), 4.23–4.28 (m, 1H, OCH), 1.50–1.78 (m, 2H, CH_2-CH_3), 1.25–1.27 (d, 3H, CH_3-CH-O), 0.95–0.99 (m, 3H, CH_3); m/z = 424.1 $(M+H)^+$ Theoretical Calculated= 423.49

7-(((5-(sec-butoxy)-1H-benzo[d]imidazol-2-yl) sulfinyl) methyl) quinolin-3-yl 2-chloroacetate (SCQD-3):

IR (KBr): 3350 (str, N–H), 3128, 3067 (str, aromatic C–H), 2934 (str, =C–H), 2877 (str, aliphatic C–H), 1731 (str, ester C=O), 1696 (str, C=N/conjugated C=C), 1596, 1557 (str, aromatic C=C), 1464 (def, CH_2/aromatic skeletal), 1382, 1342, 1311 (def, CH_2/CH), 1262, 1205 (str, ester/aryl C–O), 1174, 1136, 1096 (str, S=O/C–O–C), 982, 948 (oop, allylic =C–H), 902 (oop, =C–H), 847, 818, 737 (oop, aromatic C–H), 670, 615 cm^{-1} (str, C–Cl/C–S/S–CH_2); ^1H NMR (400 MHz, DMSO): δ 11.37 (bs, 1H, NH), 8.58 (d, 1H, H-C2 of quinoline), 6.92–7.94 (m, 7H, Ar-H), 4.54 (bs, 2H, $SOCH_2$), 4.24–4.25 (m, 1H, OCH), 4.23 (bs, 2H, CH_2Cl, overlapped), 1.50–1.75 (m, 2H, CH_2-CH_3), 1.25 (d, 3H, CH_3-CH-O), 0.97 (m, 3H, CH_3); m/z = 473.90 $(M+2)^+$ Theoretical Calculated= 471.96

7-(((5-(sec-butoxy)-1H-benzo[d]imidazol-2-yl) sulfinyl) methyl) quinolin-3-yl benzoate (SBQD-4):

IR (KBr): 3392 (str, N–H), 3069 (str, aromatic C–H), 2961 (str, =C–H), 2833 (str, aliphatic C–H), 1739 (str, ester C=O), 1620 (str, C=N/conjugated C=C), 1600, 1563, 1505 (str, aromatic C=C), 1427 (def, CH_2/aromatic skeletal), 1374, 1338 (def, CH_2/CH), 1295, 1245 (str, ester/aryl C–O), 1137, 1072 (str, S=O/C–O–C), 993, 945 (oop, allylic =C–H), 916 (oop, =C–H), 886, 848, 807, 741 (oop, aromatic C–H), 665, 616 cm^{-1} (str, C–S/S–CH_2); ^1H NMR (400 MHz, DMSO): δ 11.36 (bs, 1H, NH), 8.60 (d, 1H, H-C2 of quinoline), 8.04–8.13 (m, 2H, Ar-H), 6.92–7.90 (m, 10H, Ar-H), 4.54 (bs, 2H, $SOCH_2$), 4.23–4.27 (m, 1H, OCH), 1.50–1.75 (m, 2H, CH_2-CH_3), 1.25 (d, 3H, CH_3-CH-O), 0.97 (m, 3H, CH_3); m/z = 500.8 $(M+H)^+$ Theoretical Calculated= 499.59

7-(((5-(sec-butoxy)-1H-benzo[d]imidazol-2-yl) sulfinyl) methyl)-3-isopropoxyquinoline (SIQD-5):

IR (KBr): 3394 (str, N–H), 3155, 3064, 3010 (str, aromatic C–H), 2928 (str, =C–H), 2884 (str, aliphatic C–H), 1681 (str,

C=N/conjugated C=C), 1597, 1533 (str, aromatic C=C), 1466 (def, CH_2/aromatic skeletal), 1393, 1346, 1314 (def, CH_2/CH), 1292, 1228 (str, ether/aryl C–O), 1175, 1073, 1041 (str, S=O/C–O–C), 996, 952 (oop, allylic =C–H), 905 (oop, =C–H), 869, 850, 818, 740 (oop, aromatic C–H), 669, 614 cm^{-1} (str, C–S/S–CH_2); ^1H NMR (400 MHz, DMSO): δ 11.37 (bs, 1H, NH), 8.46–8.47 (d, 1H, H-C2 of quinoline), 6.94–7.87 (m, 7H, Ar-H), 4.58–4.65 (m, 1H, OCH), 4.54 (bs, 2H, $SOCH_2$), 4.26–4.27 (m, 1H, OCH), 1.50–1.75 (m, 2H, CH_2-CH_3), 1.31 (d, 6H, CH_3 of isopropyl group), 1.25 (d, 3H, CH_3-CH-O), 0.97 (m, 3H, CH_3); m/z = 438.8 $(M+H)^+$ Theoretical Calculated= 437.56

3-(allyloxy)-7-(((5-(sec-butoxy)-1H-benzo[d]imidazol-2-yl) sulfinyl) methyl) quinoline (SAlQD-6):

IR (KBr): 3374 (str, N–H), 3067 (str, aromatic C–H), 2943 (str, =C–H), 2884, 2833 (str, aliphatic C–H), 1681 (str, C=N/conjugated C=C), 1598, 1557, 1507 (str, aromatic C=C), 1469 (def, CH_2/aromatic skeletal), 1390, 1343, 1321, 1300 (def, CH_2/CH), 1292, 1224 (str, ether/aryl C–O), 1127 (str, S=O/C–O–C), 995, 947 (oop, allylic =C–H), 925 (oop, =C–H), 878, 852, 774 (oop, aromatic C–H), 665, 614 cm^{-1} (str, C–S/S–CH_2); ^1H NMR (400 MHz, DMSO): δ 11.37 (bs, 1H, NH), 8.46–8.47 (d, 1H, H-C2 of quinoline), 6.94–7.87 (m, 7H, Ar-H), 6.03–6.05 (m, 1H, CH of allyl), 5.47 (m, 1H, CH_2 of allyl), 5.08–5.12 (m, 1H, CH_2 of allyl), 4.74–4.75 (m, 2H, OCH_2-CH=CH_2), 4.54 (bs, 2H, $SOCH_2$), 4.27 (m, 1H, OCH), 1.37–1.89 (m, 2H, CH_2-CH_3), 1.25–1.27 (d, 3H, CH_3-CH-O), 0.97–0.99 (m, 3H, CH_3); m/z = 436.6 $(M+H)^+$ Theoretical Calculated= 435.54

Molecular Docking & Binding Interaction Analysis:

All synthesized derivatives and TU-572 were evaluated under identical molecular docking conditions against the catalytic domain of CD45 using AutoDock Vina. Binding affinity, predicted inhibitory constant (pKi) and ligand efficiency (LE) were considered for comparative analysis. The synthesized derivatives exhibited predicted binding affinities ranging from approximately −6.6 to −8.6 kcal/mol, whereas TU-572 showed a predicted binding affinity of −6.2 kcal/mol under the same docking protocol.

Based on the predicted binding affinity, five compounds were identified as the most promising computational candidates: NSQD-6 (−8.6 kcal/mol), NBQD-5 (−8.5 kcal/mol), SBQD-4 (−8.4 kcal/mol), IPQD-4 (−8.0 kcal/mol) and BBQD-4 (−7.7 kcal/mol). Their corresponding predicted Ki values were 0.506, 0.599, 0.709, 1.392 and 2.307 μM, respectively.

The ligand-efficiency analysis further supported NSQD-6, NBQD-5 and SBQD-4, with LE values of 0.239, 0.243 and 0.233, respectively. These findings indicate that the improved predicted binding affinity of the leading derivatives was accompanied, in several cases, by favourable ligand efficiency rather than being solely attributable to increased molecular size.

Analysis of the docking poses showed that the top-ranked derivatives occupied the catalytic binding region and established multiple interactions with residues surrounding the active site. NSQD-6 formed conventional hydrogen-bond interactions with LYS736, ASN735, ARG657, ARG734 and ALA830, accompanied by additional non-covalent interactions involving ASP796, SER829, VAL832, ARG704, HIS797 and TYR658. NBQD-5 showed interactions involving LYS736, ARG734, ALA830, ASN735, SER829, ARG834, ARG704, HIS797 and TYR658. SBQD-4 similarly displayed an extensive interaction network involving LYS736, ARG704, ALA830, SER829, ASN735, ARG734, HIS797, ARG834 and TYR658. **Table No.3** gives brief information about binding affinity, predicted inhibitory constant (pKi) and Ligand efficiency (LE). **Figure 2** gives 3D and 2D interactions of top-5 ranked based on the binding affinity (Kcal/mol). Overall, the identical docking protocol used for all compounds provides a

comparative basis for prioritization, while the absence of experimental biological data necessitates further validation.

ADMET Analysis and Drug-likeness

The synthesized derivatives and TU-572 were subjected to in silico ADMET and drug-likeness assessment using SwissADME. The analysis considered physicochemical properties, gastrointestinal absorption, blood–brain barrier permeability, P-glycoprotein substrate status, skin permeability and commonly used drug-likeness filters.

The top-ranked compounds showed different ADMET profiles despite their favourable docking scores. NBQD-5 displayed a consensus LogP of 4.86, TPSA of 113.38 Å², low predicted gastrointestinal absorption and was predicted to be a P-glycoprotein substrate. NSQD-6 showed a consensus LogP of 4.59, TPSA of 133.61 Å², low predicted gastrointestinal absorption and P-glycoprotein substrate status. These findings indicate that strong predicted target binding was not uniformly accompanied by favourable predicted pharmacokinetic characteristics.

Accordingly, the docking and ADMET results together provide a rational basis for carrying out biological evaluation rather than selecting candidates solely according to docking score.

Discussion

The present study employed a bioisosteric modification strategy based on the reported CD45 tyrosine phosphatase inhibitor TU-572 to explore structural features that may improve predicted interaction with the catalytic domain of CD45. TU-572 was selected as the reference scaffold because of its reported CD45 inhibitory activity, while its limited investigation in relation to broader biological and pharmacokinetic characteristics provided a rationale for further structural optimization.

The docking results demonstrated that several of the synthesized derivatives showed more favourable predicted binding affinities than TU-572. The reference molecule showed a predicted affinity of −6.2 kcal/mol, whereas the five leading derivatives exhibited values between −7.7 and −8.6 kcal/mol. The ranking was NSQD-6 > NBQD-5 > SBQD-4 > IPQD-4 > BBQD-4. This improvement suggests that modification of the parent scaffold can substantially alter the predicted accommodation of the ligand within the CD45 catalytic binding region.

Among the derivatives, NSQD-6 emerged as the highest-ranked compound, with a predicted binding affinity of −8.6 kcal/mol and predicted Ki of 0.506 μM. Its docking pose showed conventional hydrogen-bond interactions involving LYS736, ASN735, ARG657, ARG734 and ALA830, together with additional interactions involving ASP796, SER829, VAL832, ARG704, HIS797 and TYR658. The presence of multiple interactions distributed around the catalytic binding region may contribute to the favourable predicted binding score.

NBQD-5, the second-ranked derivative, displayed a predicted binding affinity of −8.5 kcal/mol and Ki of 0.599 μM. It formed interactions with LYS736, ARG734, ALA830 and ASN735, together with additional contacts involving SER829, ARG834, ARG704, HIS797 and TYR658. The extensive overlap of interacting residues between NSQD-6 and NBQD-5 suggests that the quinoline-containing scaffold and the substituted aromatic region can be accommodated within a similar portion of the CD45 binding site.

SBQD-4 also demonstrated a strong predicted binding profile, with an affinity of −8.4 kcal/mol and Ki of 0.709 μM. Its interaction pattern included LYS736, ARG704, ALA830, SER829, ASN735, ARG734, HIS797, ARG834 and TYR658. Thus, SBQD-4 retained several of the interactions observed for the two highest-ranked N-series derivatives despite incorporating the sec-butoxy substitution.

The remaining two compounds in the top five, IPQD-4 and BBQD-4, showed predicted binding affinities of −8.0 and −7.7 kcal/mol, respectively. Their inclusion among the five highest-ranked derivatives indicates that the phenyl-containing substituent at the quinoline region can also favourably contribute to the

predicted binding orientation. However, their predicted affinities were weaker than those of NSQD-6, NBQD-5 and SBQD-4. BBQD-4 showed a predicted Ki of 2.307 μM, illustrating the progressive difference in predicted affinity within the top-five group.

Comparison with the remaining derivatives demonstrates that docking performance was strongly dependent on the nature and positioning of the substituents. For example, NAQD-1, SAQD-1 and SFQD-2 showed predicted affinities of −7.1, −7.1 and −7.3 kcal/mol, respectively, while several other derivatives exhibited affinities around −6.6 to −7.0 kcal/mol. Therefore, the top five were distinguished not merely by belonging to a particular structural series but by achieving a combination of favourable predicted binding affinity and interaction patterns.

An important observation was the difference between binding affinity and ligand efficiency. Although NSQD-6 had the strongest predicted binding affinity, NBQD-5 showed a slightly higher ligand efficiency (0.243 versus 0.239 for NSQD-6). SBQD-4 also showed favourable ligand efficiency (0.233). This indicates that the ranking based exclusively on binding affinity should not be interpreted as a definitive ranking of biological potency. Instead, binding affinity, ligand efficiency, physicochemical properties and ADMET characteristics should be considered together when selecting compounds for experimental evaluation.

The ADMET analysis further demonstrates the importance of this integrated selection strategy. The top-ranked compounds did not uniformly possess superior predicted pharmacokinetic characteristics. NBQD-5 showed low predicted gastrointestinal absorption, no predicted BBB penetration and P-glycoprotein substrate status, with a consensus LogP of 4.86 and TPSA of 113.38 Å². NSQD-6 similarly showed low predicted gastrointestinal absorption, no predicted BBB penetration and P-glycoprotein substrate status, with a consensus LogP of 4.59 and TPSA of 133.61 Å².

This comparison highlights an important structure–property relationship within the series. Increasing aromatic and ester-containing substitution appears to improve the predicted interaction with the CD45 binding region in selected derivatives, but these modifications may simultaneously increase molecular size, lipophilicity and polar surface area. Consequently, improved docking scores do not necessarily translate into improved overall drug-likeness or pharmacokinetic behaviour.

The results also show why the top five should be regarded as lead candidates for biological investigation rather than confirmed CD45 inhibitors. Molecular docking provides a structural hypothesis regarding ligand–protein recognition, whereas enzymatic inhibition must be established experimentally. The docking protocol itself was designed for comparative assessment, and the authors note that conventional ligand re-docking was not possible because the active site contains a peptide residue rather than a small-molecule inhibitor. Therefore, the present computational findings should be validated through an experimental CD45 phosphatase inhibition assay, followed by selectivity and cellular studies for compounds demonstrating meaningful enzyme inhibition.

Overall, the combined docking and ADMET analysis support NSQD-6, NBQD-5, SBQD-4, IPQD-4 and BBQD-4 as a prioritized set for biological evaluation. NSQD-6 is the primary computational lead based on binding affinity, while NBQD-5 and SBQD-4 provide particularly interesting alternatives because of their favourable ligand-efficiency values. The final lead selection, however, should be determined only after experimental confirmation of CD45 inhibition and assessment of the corresponding pharmacological and safety profiles.

Conclusion

The present study describes the design, synthesis, characterization, ADMET profiling and molecular docking evaluation of 24 bioisosteric derivatives based on the TU-572 scaffold as potential CD45 tyrosine phosphatase inhibitors. The synthesized compounds were successfully characterized by

spectroscopic and mass spectrometric techniques, supporting the proposed chemical structures.

Molecular docking identified five derivatives, NSQD-6, NBQD-5, SBQD-4, IPQD-4 and BBQD-4, as the most promising computational candidates, with predicted binding affinities superior to that of the reference compound TU-572 under the applied docking conditions. NSQD-6 exhibited the most favourable predicted binding affinity (−8.6 kcal/mol), followed by NBQD-5 (−8.5 kcal/mol), SBQD-4 (−8.4 kcal/mol), IPQD-4 (−8.0 kcal/mol) and BBQD-4 (−7.7 kcal/mol). The favourable docking profiles were associated with multiple interactions within the CD45 catalytic binding region.

The ADMET assessment, however, demonstrated that improved predicted target binding was not uniformly accompanied by favourable pharmacokinetic characteristics. Therefore, docking affinity alone cannot be considered sufficient for lead selection. An integrated assessment of binding affinity, ligand efficiency, physicochemical properties and predicted ADMET characteristics is required for rational prioritization of candidates.

Taken together, the findings identify a focused group of derivatives with promising *in silico* profiles and provide a rational basis for their further investigation. **Experimental biological evaluation is now required to determine their actual CD45 tyrosine phosphatase inhibitory activity**, preferably beginning with an in vitro enzyme inhibition assay and subsequently extending to selectivity and cell-based studies for the most active compounds. Such studies will establish whether the favourable computational interactions observed for the top-ranked derivatives translate into measurable biological activity and will help determine their potential as lead structures for further CD45-targeted drug discovery.

Author Contributions: All authors have equally contributed in the preparation of the manuscript.

Affiliation:

Savitribai Phule Pune University, Pune, Maharashtra, India

Conflicts of Interest: The authors declare no conflict of interest.

Funding: The authors declare no involvement of the funding from any source.

Institutional Review Board Statement: Not applicable.

Informed Consent Statement: Not applicable.

Data Availability Statement: Data are available in the manuscript.

Acknowledgement:

The authors sincerely acknowledge Savitribai Phule Pune University (SPPU), Pune, Maharashtra, India, for providing academic support and the management of Sinhgad Technical Education Society's for an institutional affiliation for carrying out the present study.

Table 2: Physicochemical Characteristics of the Synthesized Bioisosteric Derivatives

Structure ID	Physical Description	Melting Point (°C)	Yield (%)	R_f	Molecular Formula	Molecular weight	No. of Heavy atoms
NAQD-1	Yellow coloured crystalline solid	170°C	75.8	0.58	$C_{22}H_{21}N_3O_4S$	423.49	30
NFQD-2	Brownish yellow coloured crystalline solid	140°C	88.2	0.68	$C_{21}H_{19}N_3O_4S$	409.46	29
NCQD-3	Yellow amorphous solid	180°C	78.2	0.52	$C_{22}H_{20}ClN_3O_4S$	457.93	31
NPQD-4	Greenish yellow colour amorphous solid	180°C	75.2	0.42	$C_{28}H_{25}N_3O_4S$	499.59	36
NBQD-5	Yellow amorphous solid	160°C	79.2	0.52	$C_{27}H_{23}N_3O_4S$	485.56	35
NSQD-6	Yellow amorphous solid flakes	160°C	79.3	0.66	$C_{27}H_{23}N_3O_5S$	501.56	36
NAlQD-7	Yellow amorphous solid flakes	140°C	73.8	0.53	$C_{23}H_{23}N_3O_3S$	421.52	30
NHQD-8	Yellow amorphous solid	130°C	88.6	0.51	$C_{20}H_{19}N_3O_3S$	381.45	27
IAQD-1	Brownish yellow waxy solid	140°C	72.1	0.68	$C_{22}H_{21}N_3O_4S$	423.49	30
IFQD-2	Brownish yellow waxy solid	150°C	78.2	0.68	$C_{21}H_{19}N_3O_4S$	409.46	29
ICQD-3	Yellowish brown waxy solid	140°C	75.3	0.59	$C_{22}H_{20}ClN_3O_4S$	457.93	31
IPQD-4	Yellowish brown waxy solid	130°C	75.2	0.54	$C_{28}H_{25}N_3O_4S$	499.60	36
IIQD-5	Brownish yellow waxy solid	150°C	70.2	0.62	$C_{23}H_{25}N_3O_3S$	423.53	30
IHQD-6	Brownish yellow amorphous solid	140°C	88.4	0.58	$C_{20}H_{19}N_3O_3S$	381.45	27
BAQD-1	Yellowish grey coloured solid	140°C	85.8	0.68	$C_{23}H_{23}N_3O_4S$	437.5	31
BFQD-2	Yellowish brown solid	120°C	85.2	0.65	$C_{22}H_{21}N_3O_4S$	423.49	30
BCQD-3	Yellowish grey coloured solid	100°C	82.4	0.52	$C_{23}H_{22}ClN_3O_4S$	471.96	32
BBQD-4	Yellowish grey coloured solid	100°C	72.8	0.52	$C_{28}H_{25}N_3O_4S$	499.59	36
SAQD-1	Yellow amorphous solid	150°C	82.4	0.58	$C_{23}H_{23}N_3O_4S$	437.51	31
SFQD-2	Yellow amorphous solid	170°C	78.6	0.60	$C_{22}H_{21}N_3O_4S$	423.49	30
SCQD-3	Brown amorphous solid	150°C	88.2	0.68	$C_{23}H_{22}ClN_3O_4S$	471.96	32
SBQD-4	Yellow amorphous solid	180°C	81.2	0.60	$C_{28}H_{25}N_3O_4S$	499.59	36
SIOD-5	Brownish yellow waxy solid	150°C	72.5	0.56	$C_{24}H_{27}N_3O_3S$	437.56	31
SAlQD-6	Yellow amorphous solid	170°C	75.0	0.60	$C_{24}H_{25}N_3O_3S$	435.54	31

Table 3: Molecular Docking Analysis and Binding Interactions of the Synthesized Bioisosteric Derivatives

Structure ID	Binding Affinity (Kcal/mol)	pKi (µM)	Ligand Efficiency	H- interactions	Other type of interactions
NAQD-1	-7.1	6.344	0.237	ARG 704[#], HIS 797[#]	LYS 736[####], ARG 704[####], ARG 657[###]
NFQD-2	-6.7	12.450	0.231	ASP 796[#], THR 792[#]	GLU 731[####], LYS 736[####], HIS 797[###], TYR 658[#####]
NCQD-3	-6.8	10.519	0.219	ARG 704[#], ARG 734[##]	LYS 736[####]
NPQD-4	-7.3	4.528	0.203	PRO 636[##], GLN 633[##], ARG 637[##]	VAL 638[###], ILE 644[###], LEU 869[#####]
NBQD-5	-8.5	0.599	0.243	LYS 736[#], ARG 734[#], ALA 830[#], ASN 735[##], SER 829[##]	ARG 834[###], ARG 704[###], HIS 797[###], TYR 658[#####]
NSQD-6	-8.6	0.506	0.239	LYS 736[#], ASN 735[#], ARG 657[#], ARG 734[#], ALA 830[#], ASP 796[##], SER 829[##]	VAL 832[###], ARG 704[####], HIS 797[####], TYR 658[#####]
NAlQD-7	-6.7	12.450	0.223	ARG 704[#], ARG 734[##]	LYS 736[####]
NHQD-8	-6.7	12.450	0.248	LYS 736[#], ASP 796[#], ARG 657[#], HIS 797[#]	ARG 704[###], ARG 734[####]
IAQD-1	-7.1	6.344	0.237	ARG 704[#]	ARG 734[####], LYS 736[####]
IFQD-2	-6.7	12.450	0.231	ARG 704[#], ARG 734[##]	ARG 657[###], LYS 736[####]
ICQD-3	-7.1	6.344	0.229	ARG 704[#], ARG 734[##]	HIS 797[###], LYS 736[####]
IPQD-4	-8.0	1.392	0.222	LYS 736[#], ALA 830[#], SER 829[##]	ARG 657[###], ARG 734[####], HIS 797[####], TYR 658[#####]
IIQD-5	-6.9	8.887	0.230	VAL 638[#]	ILE 644[###], LEU 869[###]
IHQD-6	-6.7	12.450	0.248	ARG 704[#], ARG 734[##]	LYS 736[####]
BAQD-1	-7.0	7.508	0.226	LYS 736[#]	GLU 731[####], HIS 797[####], ILE 661[###], ALA 830[###], TYR 658[###]
BFQD-2	-6.6	14.736	0.220	ARG 728[#], GLU 731[##]	ALA 830[###], TYR 658[####], LYS 736[####], HIS 797[####]
BCQD-3	-6.6	14.736	0.206	ARG 637[#], ARG 864[#]	LEU 869[###], VAL 638[####]
BBQD-4	-7.7	2.307	0.214	LYS 736[#]	ARG 657[###], ARG 704[###], ARG 734[####], GLU 731[####]
SAQD-1	-7.1	6.344	0.229	ARG 704[#]	ARG734[####], LYS 736[####]
SFQD-2	-7.3	4.528	0.243	LYS 736[#], ARG 704[#], ALA830[#], SER 829[##]	ARG834[###], ARG734[####], HIS 797[####], TYR 658[#####]
SCQD-3	-6.9	8.887	0.216	ARG 637[#]	LEU 869[###], VAL 638[####]
SBQD-4	-8.4	0.709	0.233	LYS 736[#], ARG 704[#], ALA830[#], SER 829[##], ASN 735[##]	ARG734[####], HIS 797[####], ARG834[###], TYR 658[#####]
SIOD-5	-6.7	12.450	0.216	LYS 736[#]	PRO 795[###], ARG 657[###], ARG 704[###], ARG 734[####]
SAlQD-6	-6.6	14.736	0.213	VAL 638[##]	PHE 632[###], ILE 644[###]
TU-572	-6.2	28.920	0.258	LYS 736[#], ASN 735[##]	ARG 734[####], ARG 657[###]

Notations: #- conventional hydrogen bond, ##- carbon hydrogen bond/ Pi-Donor Hydrogen Bond, ###- Alkyl/ Pi-Alkyl ####- Pi-Cation/Pi-Anion/Pi-Sigma #####- Pi-Pi shaped/Stacd

Table 4: *In Silico* ADMET and Drug-Likeness Profiles of the Synthesized Bioisosteric Derivatives

Structure ID	Log S	Consensus Log P	nHA	nHD	nR	TPSA	GI absorption	BBB	P-gp substrate	Log Kp (cm/s)	Lipinski	Ghose	Veber	Egan	Muegge	BA Score	PAINS	BRENK
NAQD-1	-4.56	3.58	6	1	8	113.38	High	No	No	-6.46	0	0	0	0	0	0.55	0	0
NFQD-2	-4.5	3.37	6	1	8	113.38	High	No	No	-6.36	0	0	0	0	0	0.55	0	1
NCQD-3	-5.09	3.98	6	1	9	113.38	Low	No	No	-6.22	0	0	0	0	0	0.55	0	1
NPQD-4	-5.95	4.91	6	1	10	113.38	Low	No	Yes	-5.78	0	3	0	1	1	0.55	0	0
NBQD-5	-5.99	4.86	6	1	9	113.38	Low	No	Yes	-5.66	0	3	0	1	1	0.55	0	0
NSQD-6	-6.2	4.59	7	2	9	133.61	Low	No	Yes	-5.61	1	3	0	1	1	0.55	0	0
NAlQD-7	-5.03	4.22	5	1	9	96.31	High	No	Yes	-5.83	0	0	0	0	0	0.55	0	1
NHQD-8	-4.42	3.29	5	2	6	107.31	High	No	Yes	-6.27	0	0	0	0	0	0.55	0	0
IAQD-1	-4.57	3.52	6	1	7	113.38	High	No	No	-6.52	0	0	0	0	0	0.55	0	0
IFQD-2	-4.51	3.31	6	1	7	113.38	High	No	No	-6.43	0	0	0	0	0	0.55	0	1
ICQD-3	-5.09	3.91	6	1	8	113.38	Low	No	No	-6.29	0	0	0	0	0	0.55	0	1
IPQD-4	-5.96	4.84	6	1	9	113.38	Low	No	Yes	-5.85	0	3	0	1	0	0.55	0	0
IIQD-5	-5.21	4.23	5	1	7	96.31	High	No	Yes	-5.8	0	1	0	0	0	0.55	0	0
IHQD-6	-4.42	3.22	5	2	5	107.31	High	No	Yes	-6.34	0	0	0	0	0	0.55	0	0
BAQD-1	-4.79	3.92	6	1	9	113.38	Low	No	Yes	-6.29	0	0	0	0	0	0.55	0	0
BFQD-2	-4.73	3.71	6	1	9	113.38	High	No	No	-6.19	0	0	0	0	0	0.55	0	1
BCQD-3	-5.32	4.32	6	1	10	113.38	Low	No	Yes	-6.05	0	0	0	0	0	0.55	0	1
BBQD-4	-6.22	5.2	6	1	10	113.38	Low	No	Yes	-5.49	0	3	0	1	1	0.55	0	0
SAQD-1	-4.91	3.9	6	1	8	113.38	Low	No	Yes	-6.23	0	0	0	0	0	0.55	0	0
SFQD-2	-4.84	3.69	6	1	8	113.38	High	No	No	-6.14	0	0	0	0	0	0.55	0	1
SCQD-3	-5.43	4.29	6	1	9	113.38	Low	No	Yes	-6	0	0	0	0	0	0.55	0	1
SBQD-4	-6.33	5.17	6	1	9	113.38	Low	No	Yes	-5.43	0	3	0	1	1	0.55	0	0
SIOD-5	-5.55	4.61	5	1	8	96.31	Low	No	Yes	-5.5	0	1	0	1	0	0.55	0	0
SAlQD-6	-5.37	4.54	5	1	9	96.31	High	No	Yes	-5.61	0	1	0	0	0	0.55	0	1
TU-572	-3.91	3.1	4	1	6	112.38	High	No	No	-6.52	0	0	0	0	0	0.55	0	0

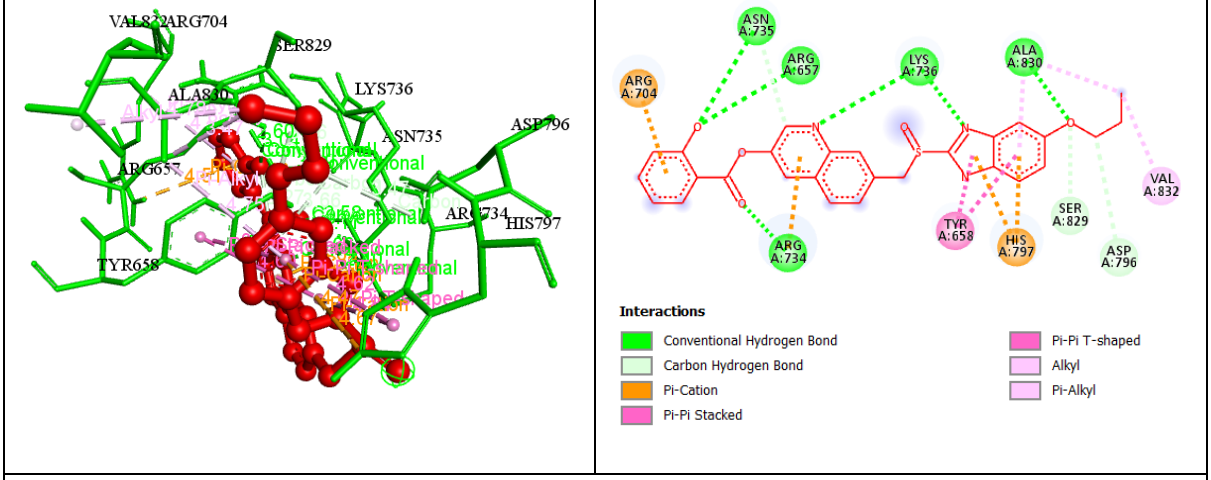

NSQD-6

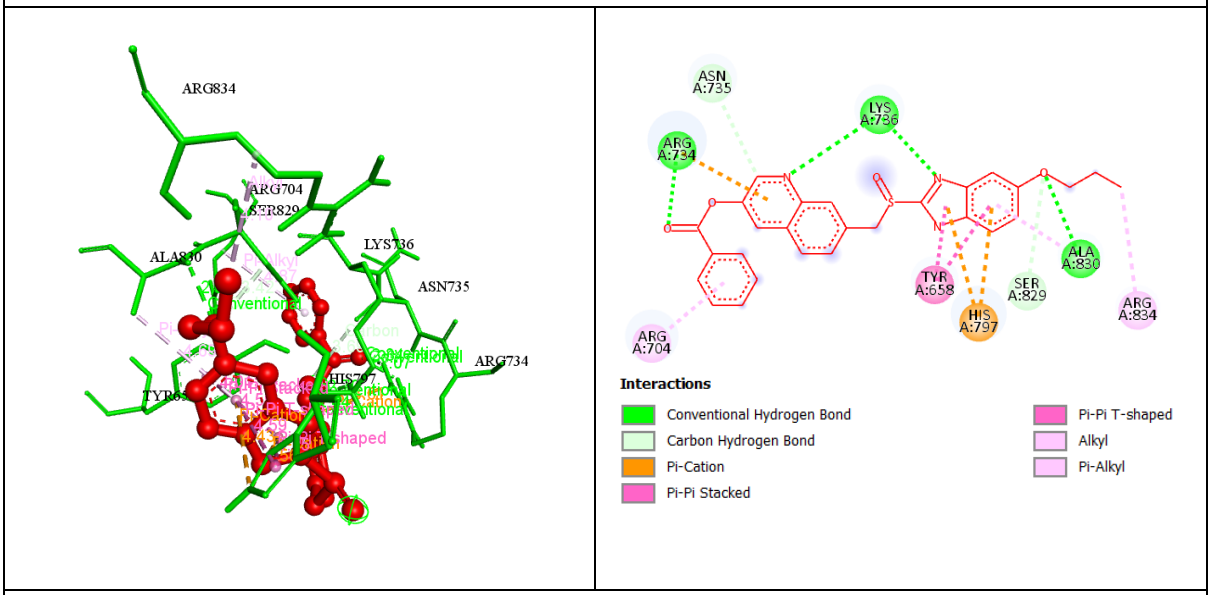

NBQD-5

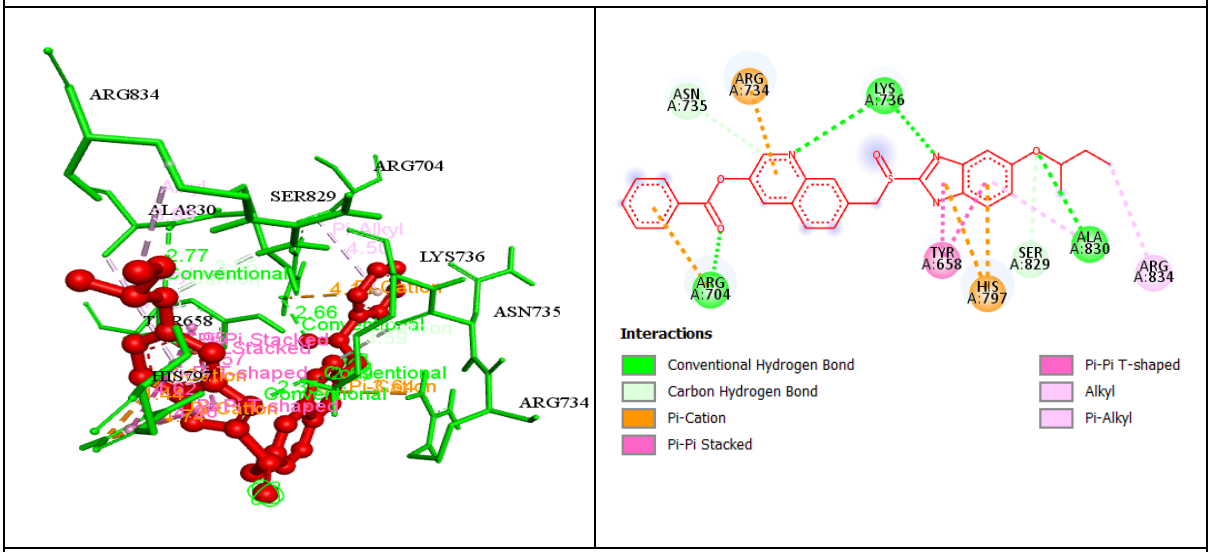

SBQD-4

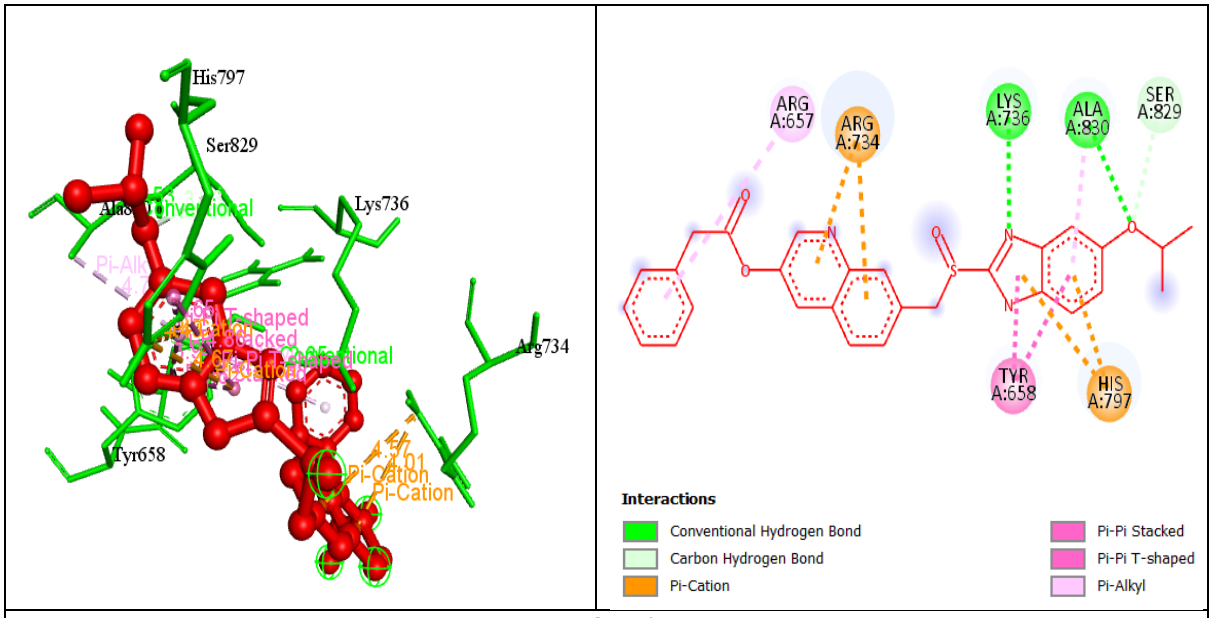

IPQD-4

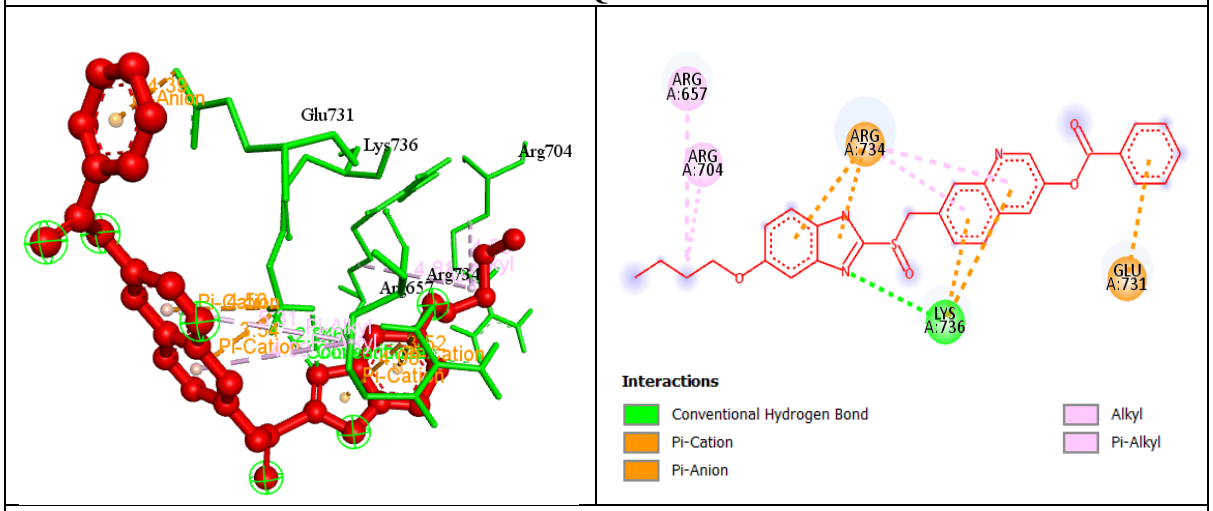

BBQD-4

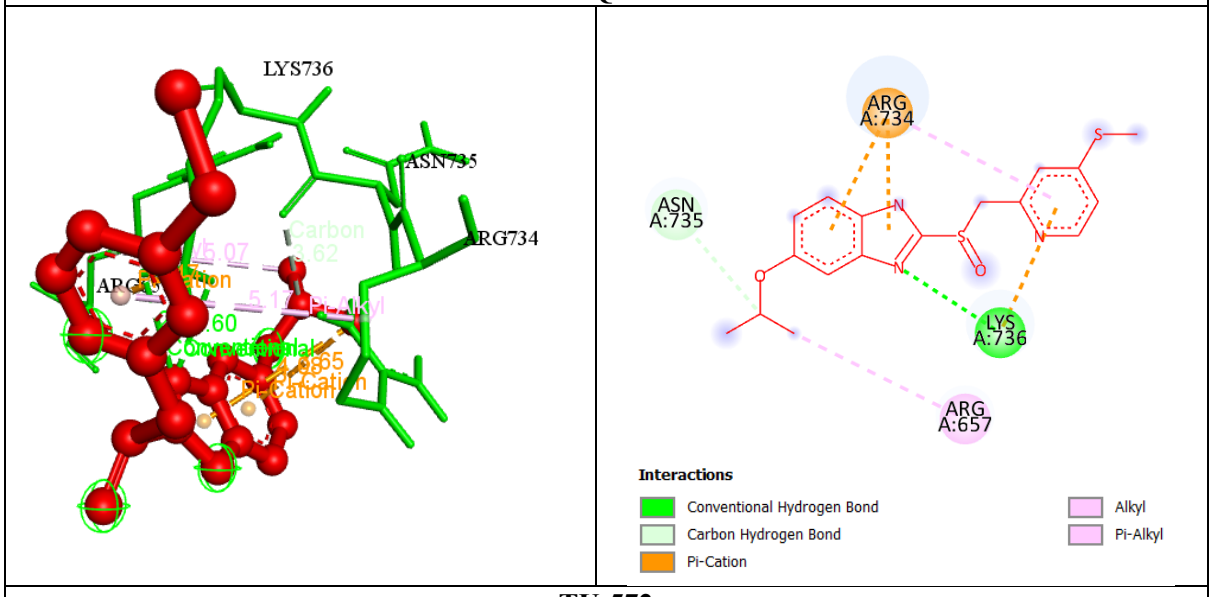

TU-572

Figure 2: 2D and 3D interactions of top-5 ranked molecules based on the binding affinity (Kcal/mol) and reference molecule.

References:

1. Al Barashdi MA, Ali A, McMullin MF, Mills K. Protein tyrosine phosphatase receptor type C (PTPRC or CD45). Journal of clinical pathology. 2021 Sep;74(9):548-52.
2. Ahmed MG, Limmer A, Hartmann M. CD45RA and CD45RO are regulated in a cell-type specific manner in inflammation and sepsis. Cells. 2023 Jul 17;12(14):1873 Gourdine JP, Nava P, Noll AJ, Duong DM, Seyfried NT, Cummings RD. CD45 and Basigin (CD147) Are Functional Ligands for Galectin-8 on Human Leukocytes. Biomolecules. 2025 Aug 27;15(9):1243.
3. Kästle M, Merten C, Hartig R, Kaehne T, Liaunardy-Jopeace A, Woessner NM, Schamel WW, James J, Minguet S, Simeoni L, Schraven B. Tyrosine 192 within the SH2 domain of the Src-protein tyrosine kinase p56Lck regulates T-cell activation independently of Lck/CD45 interactions. Cell Communication and Signaling. 2020 Nov 23;18(1):183.
4. Goyette J, Nieves DJ, Ma Y, Gaus K. How does T cell receptor clustering impact on signal transduction? Journal of cell science. 2019 Feb 15;132(4): jcs226423.
5. Cong R, Yang J, Zhou J, Shi J, Zhu Y, Zhu J, Xiao J, Wang P, He Y, He B. The potential role of protein tyrosine phosphatase, receptor type C (CD45) in the intestinal ischemia–reperfusion injury. Journal of Computational Biology. 2020 Aug 1;27(8):1303-12.
6. Liu R, Mathieu C, Berthelet J, Zhang W, Dupret JM, Rodrigues Lima F. Human protein tyrosine phosphatase 1B (PTP1B): from structure to clinical inhibitor perspectives. International Journal of Molecular Sciences. 2022 Jun 24;23(13):7027.
7. Kobayashi-Matsunaga Y, Ishii T, Hamaguchi T, Osada H, Sato M. Synthesis and characterization of a novel protein tyrosine phosphatase inhibitor, 2-(cyclobutylamino)-N-(2-furylmethyl)-2-thioxoacetamide. Letters in Drug Design & Discovery. 2005 May 1;2(3):224-7.
8. Hamaguchi T, Takahashi A, Kagamizono T, Manaka A, Sato M, Osada H. Synthesis and characterization of a potent and selective protein tyrosine phosphatase inhibitor, 2-[(4-methylthiopyridin-2-yl) methylsulfinyl] benzimidazole. Bioorganic & medicinal chemistry letters. 2000 Dec 4;10(23):2657-60.
9. Urbanek RA, Suchard SJ, Steelman GB, Knappenberger KS, Sygowski LA, Veale CA, Chapdelaine MJ. Potent reversible inhibitors of the protein tyrosine phosphatase CD45. Journal of medicinal chemistry. 2001 May 24;44(11):1777-93.
10. Beers SA, Malloy EA, Wu W, Wachter MP, Gunnia U, Cavender D, Harris C, Davis J, Brosius R, Pellegrino-Gensey JL, Siekierka J. Nitroarylhydroxymethylphosphonic acids as inhibitors of CD45. Bioorganic & medicinal chemistry. 1997 Dec 1;5(12):2203-11.
11. Heneberg P. Use of protein tyrosine phosphatase inhibitors as promising targeted therapeutic drugs. Current medicinal chemistry. 2009 Feb 1;16(6):706-33.
12. Kuban-Jankowska A, Gorska M, Tuszynski JA, Churchill CD, Winter P, Klobukowski M, Wozniak M. Inactivation of protein tyrosine phosphatases by peracids correlates with the hydrocarbon chain length. Cellular Physiology and Biochemistry. 2015 Jun 1;36(3):1069-83.

13. Li WR, Lin ST, Hsu NM, Chern MS. Efficient total synthesis of pulchellalactam, a CD45 protein tyrosine phosphatase inhibitor. The Journal of organic chemistry. 2002 Jul 12;67(14):4702-6.

14. Burke Jr TR, Zhang ZY. Protein–tyrosine phosphatases: structure, mechanism, and inhibitor discovery. Peptide Science. 1998;47(3):225-41.

15. Desmarais S, Jia Z, Ramachandran C. Inhibition of protein tyrosine phosphatases PTP1B and CD45 by sulfotyrosyl peptides. Archives of biochemistry and biophysics. 1998 Jun 15;354(2):225-31.

16. Tautz L, Mustelin T. Strategies for developing protein tyrosine phosphatase inhibitors. Methods. 2007 Jul 1;42(3):250-60.

17. He R, Zeng LF, He Y, Zhang S, Zhang ZY. Small molecule tools for functional interrogation of protein tyrosine phosphatases. The FEBS journal. 2013 Jan;280(2):731-50.

18. Nam, H., Poy, F., Saito, H., & Frederick, C. A. (2005). *Crystal structure of the tandem phosphatase domains of RPTP CD45 with a pTyr peptide* (PDB ID: 1YGU). RCSB Protein Data Bank. https://doi.org/10.2210/pdb1YGU/pdb

19. Dassault Systèmes BIOVIA. (2024). *BIOVIA Discovery Studio* (Version 2024) [Computer software].

20. Eberhardt, Jerome, Santos-Martins, Diogo, Tillack, Andreas F., Forli, Stefano, & Olson, Arthur J. (2021). AutoDock Vina 1.2.0: New docking methods, expanded force field, and Python bindings. *Journal of Chemical Information and Modeling, 61*(8), 3891–3898. https://doi.org/10.1021/acs.jcim.1c00203

21. Revvity Signals Software, Inc. (2024). *ChemDraw Professional* (Version 24.0) [Computer software].

22. Ramos RS, Borges RS, de Souza JS, Araujo IF, Chaves MH, Santos CB. Identification of potential antiviral inhibitors from hydroxychloroquine and 1, 2, 4, 5-tetraoxanes analogues and investigation of the mechanism of action in SARS-CoV-2. International Journal of Molecular Sciences. 2022 Feb 4;23(3):1781.

23. Elhady SS, Alshobaki NM, Elfaky MA, Koshak AE, Alharbi M, Abdelhameed RF, Darwish KM. Deciphering molecular aspects of potential α-glucosidase inhibitors within Aspergillus terreus: A computational odyssey of molecular docking-coupled dynamics simulations and pharmacokinetic profiling. Metabolites. 2023 Aug 12;13(8):942.

24. Daina A, Michielin O, Zoete V. SwissADME: a free web tool to evaluate pharmacokinetics, drug-likeness and medicinal chemistry friendliness of small molecules. Scientific Reports. 2017; 7: 42717.